JOURNAL OF THEORETICAL
AND APPLIED MECHANICS
3, **36**, 1998

CONSOLIDATION OF A POROUS MULTILAYERED SUBSOIL UNDERGOING LARGE DEFORMATION

Gwidon Szefer

Marian Mikołajek

Institute of Structural Mechanics, Cracow University of Technology
e-mail: szefer@limba.wil.pk.edu.pl

In the paper the process of deformation of an elastic porous skeleton at finite strains and the associated transport of fluid through the pores is considered. Undergoing large deformations these coupled interaction phenomena require skilful analysis. Numerical results for a three-layered subsoil resting on a rigid foundation under different permeability conditions in the uni-axial state of strains are given.

Key words: consolidation, porous skeleton, separation, large deformation

1. Introduction

Consolidation processes which arise in many problems of geotechnics, environmental engineering, biomechanics, chemical industry etc., need improved understanding of transport and interaction phenomena in porous, fluid saturated media. These phenomena being very complex in different bodies (e.g. pollutant soils, dampers, bones) can be analysed precisely when large deformations and large displacements are not ignored.

In the present paper the consolidation of a multilayred foundation consisting of an elastic porous skeleton and inviscid, incompressible fluid is considered. Large deformations and hence separation of the fluid and solid particles, change of porosity, and configuration dependent permeability are taken into account. Consequent lagrangian descriptions for both the solid as well as the fluid phase have been used. The finite strain formulation leads to many nontrivial computational details which require careful analysis and inspection. The paper aims at presentation of numerical results for a quasi-stationary nonlinear consolidation process in the uniaxial state of strains. A general description of the problem is based on the model presented by Szefer (1980), (1998).

2. Formulation of the problem

Consider a two-component porous body with a linear elastic skeleton, undergoing consolidation due to a static load acting on the boundary. Using the following denotation

$\boldsymbol{u}^s, \mathbf{E}, \mathbf{S}$	–	displacement vector, strain tensor and the II Piola-Kirchhoff stress tensor for the skeleton particle
$\boldsymbol{u}^F, \boldsymbol{F}^{-1,F}, p$	–	displacement, deformation gradient and pressure, respectively, for the fluid component
$n, \theta, \boldsymbol{\tau}$	–	porosity, fluid content ratio and interaction drag vector, respectively

one can write the system of governing equations in material coordinates as follows:

— balance of mass for the fluid

$$nJ^F = n_0$$

— balance of momentum

$$\begin{aligned} &[(1-n_0)S_{KL}(\delta_{iL}+u^s_{i,L}) - nJ^F pX^F_{K,i}]_{,K} = 0 \\ &-n[J^F pX^F_{K,i}]_{,K} + \tau_i = 0 \end{aligned} \tag{2.1}$$

— kinematical relations

$$E_{KL} = \frac{1}{2}(u^s_{K,L} + u^s_{L,K} + u^s_{N,K}u^s_{N,L})$$

$$\theta = nJ^s - n_0$$

— constitutive relationships

$$S_{KL} = \frac{1-n}{1-n_0}[2NE_{KL} + (AE_{NN} + Q\theta)\delta_{KL}]$$

$$p = QE_{KK} - R\theta \qquad \tau_i = \frac{1}{k}(v^F_i - v^s_i)$$

where

v_i^α	–	velocities
cof	–	algebraic co-factor
k	–	coefficient of permeability
N, A, Q, R	–	material constants
n_0	–	initial porosity

and

$$X^F_{K,i} = \frac{1}{J^F} \operatorname{cof}\,(\delta_{iK} + u^F_{i,K}) \qquad J^\alpha = \det(\delta_{iK} + u^\alpha_{i,K}) \qquad \alpha = s, F$$

In Eq $(2.1)_1$ we leave out the mass balance for the solid (since it determines the skeleton mass density which is not coupled with the remaining equations) whereas in $(2.1)_{2,3}$ we neglect the body forces.

The system (2.1) should be complemented by suitable initial and boundary conditions

$$\begin{aligned}
&u^\alpha_K(\boldsymbol{X}, t_0) = u^\alpha_{K0}(\boldsymbol{X}) && \boldsymbol{X} \in B_R \qquad \alpha = s, F\\
&\dot{u}^\alpha_K(\boldsymbol{X}, t_0) = v^\alpha_{K0}(\boldsymbol{X}) && \\
&(1 - n_0) S_{KL}(\delta_{iL} + u^s_{i,L}) N_K = q_{Ri}(\boldsymbol{X}_0, t) && \boldsymbol{X}_0 \in S_\sigma\\
&-nJ^F p X^F_{K,i} N_K = p_{Ri}(\boldsymbol{X}_0, t) && \text{for permeable edge}\\
&u^s_K(\boldsymbol{X}_0, t_0) = g(\boldsymbol{X}_0, t) && \boldsymbol{X}_0 \in S_u \qquad S_R = S_\sigma \cup S_u\\
&(v^F_i - v^s_i) n_i = 0 && \text{for impermeable edge}
\end{aligned} \tag{2.2}$$

N_K and n_i – stand for the components of unit outward normal vectors in the reference and current configurations, respectively.

3. One-dimensional process of consolidation

Consider a three-layered subsoil resting on a rigid stratum loaded uniformly on the upper surface by the load $q(t)$ (Fig.1). Taking Z for the lagrangian and z^s, z^F for the current coordinates of the particles, let us denote the list of unknown functions describing the one-dimensional case by

W, U	–	displacements of the solid and fluid particles, respectively
E_{ZZ}, S_{ZZ}	–	strain and stress components in the solid
p	–	fluid pressure
τ_z	–	diffusive drag force
n, θ	–	porosity and fluid content ratio.

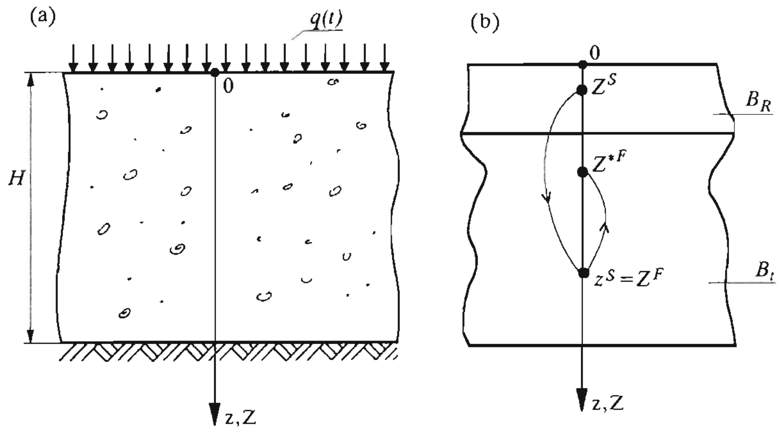

Fig. 1.

Thus it we have

$$
\begin{aligned}
z^s &= Z + W(Z,t) & J^s &= 1 + \frac{\partial W}{\partial Z} & v^s &= \frac{\partial W}{\partial t} \\
z^F &= Z + U(Z,t) & J^F &= 1 + \frac{\partial U}{\partial Z} & v^F &= \frac{\partial U}{\partial t} \\
\frac{\partial Z}{\partial z^F} &= \frac{1}{1 + \frac{\partial U}{\partial Z}}
\end{aligned}
\tag{3.1}
$$

Hence the system of governing equations for the one-dimensional case is

$$
\begin{aligned}
& n\Big(1 + \frac{\partial U}{\partial Z}\Big) = n_0 && \frac{\partial}{\partial Z}\Big[(1-n_0)S_{ZZ}\Big(1 + \frac{\partial W}{\partial Z}\Big) - np(Z^*,t)\Big] = 0 \\
& \theta = n(1 + \frac{\partial W}{\partial Z}\Big) - n_0 && - n\frac{\partial p}{\partial Z} + \tau_Z = 0 \\
& E_{ZZ} = \frac{\partial W}{\partial Z} + \frac{1}{2}\Big(\frac{\partial W}{\partial Z}\Big)^2 && S_{ZZ} = (2N + A)E_{ZZ} + Q\theta \\
& p = QE_{ZZ} + R\theta && \tau_Z = \frac{1}{k}[v^F(Z^*,t) - v^s(Z,t)]
\end{aligned}
\tag{3.2}
$$

It should be emphasized, that the fluid and solid particles beeing in contact at the instant t have different coordinates Z^* and Z in the reference configuration (see Fig.1). The coordinate Z^* results from the implicit relationship

$$
Z^*: \quad z^F = z^s \Rightarrow Z^* + U(Z^*,t) = Z^s + W(Z^s,t) \tag{3.3}
$$

(see also the companion paper of Szefer).

This fact constitutes an important part of the numerical analysis by using the material description.

A weak formulation of the governing equations can be stated by applying Galerkin's procedure of weighted residuals (Lewis and Schrefler, 1987) or by using the virtual power formalism. Using the latter approach yields

$$\begin{gathered}\int\limits_0^H \Big[(1-n_0)S_{ZZ}\Big(1+\frac{\partial W}{\partial Z}\Big)\frac{\partial}{\partial Z}(\delta W)+np\frac{\partial}{\partial Z}(\delta U)+\frac{\partial n}{\partial Z}p(\delta U-\delta W)\Big]\,dZ+ \\ +\int\limits_0^H \tau_Z(\delta U-\delta W)\,dZ=(1-n_0)q(t)\delta W(0,t)\end{gathered} \tag{3.4}$$

where δW, δU – stand for the virtual displacements.

To overcome the nonlinearities appearing in the model described by Eq (3.4) the incremental procedure of step-by-step linearization has been used.

Thus, approximating the field variables in space as usual by the finite element techniques and by the weighted finite difference discretization in the time domain one obtains the matrix equation

$$(\mathsf{K}^s+\mathsf{K}^F)\Delta\hat{\boldsymbol{U}}=\Delta\boldsymbol{F}+\boldsymbol{Q}_t \tag{3.5}$$

at each step of the time instant t, where

$\Delta\hat{\boldsymbol{U}}$	–	nodal displacement vector of the increments
$\mathsf{K}^s, \mathsf{K}^F$	–	stiffnes matrices resulting from the solid and fluid components, respectively
$\Delta\boldsymbol{F}$	–	vector of the external force increment
$\boldsymbol{Q}_t$	–	residual vector resulting from linearization of the nonlinear terms.

4. Numerical examples

We will focus our attention on the three layered foundation resting on the rigid base (Fig.2).

For numerical solution, the time discretization proceeds according to the scheme

$$u^\alpha_{t+\Delta t}=u^\alpha_t+[(1-\delta)\dot{u}_t+\delta\dot{u}_{t+\Delta t}]\Delta t\Rightarrow \dot{u}_{t+\Delta t}=\frac{\Delta u^\alpha}{\delta\Delta t}-\frac{1-\delta}{\delta}\dot{u}^\alpha_t$$

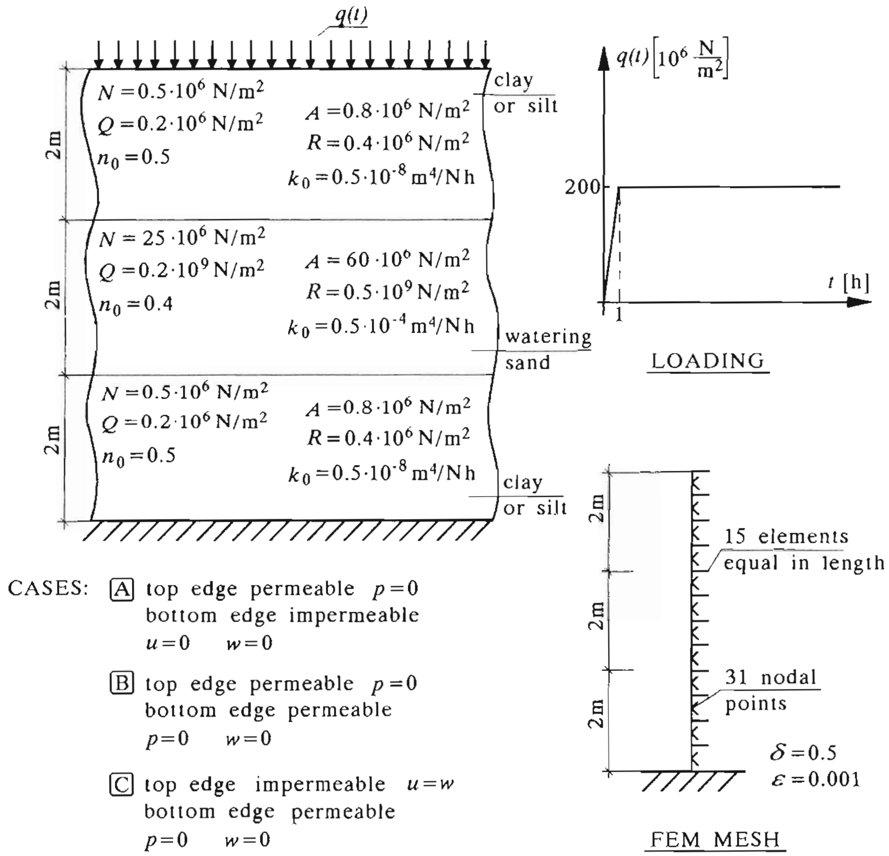

Fig. 2.

where $0 < \delta < 1$, $\alpha = s, F$.

Thus, the diffusive drag force (3.2) has the form

$$\tau_Z(t+\Delta t) = \frac{1}{k\delta}\Big(\frac{\Delta U}{\Delta t} - \frac{\Delta W}{\Delta t}\Big) - \frac{1-\delta}{k\delta}(\dot{U}_t - \dot{W}_t) \tag{4.1}$$

Applying the finite element method we will use one dimensional isoparametric finite elements. Then the displacement increments of the skeleton and fluid are

$$\begin{aligned}[\Delta W] &= [\phi_i, 0, \phi_j, 0, \phi_m, 0][\Delta\hat{w}_i, \Delta\hat{u}_i, \Delta\hat{w}_j, \Delta\hat{u}_j, \Delta\hat{w}_m, \Delta\hat{u}_m]^\top = \boldsymbol{\phi}^s \Delta\hat{\boldsymbol{u}} \\ [\Delta U] &= [0, \phi_i, 0, \phi_j, 0, \phi_m][\Delta\hat{w}_i, \Delta\hat{u}_i, \Delta\hat{w}_j, \Delta\hat{u}_j, \Delta\hat{w}_m, \Delta\hat{u}_m]^\top = \boldsymbol{\phi}^F \Delta\hat{\boldsymbol{u}}\end{aligned} \tag{4.2}$$

where

$$\phi_i(\xi) = \frac{1}{2}\xi^2 - \frac{1}{2}\xi \qquad \phi_j(\xi) = 1 - \xi^2 \qquad \phi_i(\xi) = \frac{1}{2}\xi^2 + \frac{1}{2}\xi$$

After introducing Eq (4.2) into Eq (3.5) the matrices may be rewritten as follows

$$\begin{aligned}
\mathbf{K}^s &= \int_{-1}^{1} \alpha_1 \boldsymbol{\phi}^{s\,\top}_{,\xi} \boldsymbol{\phi}^s_{,\xi} J^{se}\, d\xi + \int_{-1}^{1} \alpha_2 \boldsymbol{\phi}^{F\,\top}_{,\xi} \boldsymbol{\phi}^s_{,\xi} J^{se}\, d\xi + \\
&+ \int_{-1}^{1} \alpha_3 \frac{1}{k\delta\Delta t} \boldsymbol{\phi}^{s\,\top} \boldsymbol{\phi}^s J^{se}\, d\xi + \int_{-1}^{1} \alpha_4 \frac{1}{k\delta\Delta t} \boldsymbol{\phi}^{s\,\top} \boldsymbol{\phi}^F J^{se}\, d\xi \\
\mathbf{K}^F &= \int_{-1}^{1} \alpha_5 \boldsymbol{\phi}^{F\,\top}_{,\xi} \boldsymbol{\phi}^F_{,\xi} J^{Fe}\, d\xi + \int_{-1}^{1} \alpha_6 \boldsymbol{\phi}^{s\,\top}_{,\xi} \boldsymbol{\phi}^F_{,\xi} J^{Fe}\, d\xi + \\
&+ \int_{-1}^{1} \alpha_7 \frac{1}{k\delta\Delta t} \boldsymbol{\phi}^{F\,\top} \boldsymbol{\phi}^F J^{Fe}\, d\xi + \int_{-1}^{1} \alpha_8 \frac{1}{k\delta\Delta t} \boldsymbol{\phi}^{F\,\top} \boldsymbol{\phi}^s J^{Fe}\, d\xi \\
\boldsymbol{Q}_t &= \frac{1-\delta}{\delta} \int_{-1}^{1} \frac{1}{k} \boldsymbol{\phi}^{s\,\top} \boldsymbol{\phi}^s \dot{W}_t J^{se}\, d\xi - \frac{1-\delta}{\delta} \int_{-1}^{1} \frac{1}{k} \boldsymbol{\phi}^{s\,\top} \boldsymbol{\phi}^F \dot{U}_t J^{se}\, d\xi + \\
&+ \frac{1-\delta}{\delta} \int_{-1}^{1} \frac{1}{k} \boldsymbol{\phi}^{F\,\top} \boldsymbol{\phi}^F \dot{U}_t J^{Fe}\, d\xi - \frac{1-\delta}{\delta} \int_{-1}^{1} \frac{1}{k} \boldsymbol{\phi}^{F\,\top} \boldsymbol{\phi}^s \dot{W}_t J^{Fe}\, d\xi
\end{aligned} \tag{4.3}$$

where $\boldsymbol{\phi}^\alpha_{,\xi}$ – matrix of derivatives

$$\alpha_1 = (1 - n_0)(2N + A - Qn) \qquad \alpha_2 = \dots$$

At this point let us notice that the global stiffness matrix is a band but asymmetric one. That is known in contact problems and here we have some kind of internal contact between the skeleton and fluid particles.

As it was mentioned before, due to the separation of fluid and skeleton particles, during the consolidation process some part of the fluid is squeezed out of the pores. Then, it is necessary (at each time step) to describe and evaluate the current fluid reference configuration, which is different from the reference configuration of the skeleton. That is realised by using an iterative procedure which occured to be fast convergent.

Denoting the current common position of particles by

$$z^{s(N+1)} = Z^s + \sum_N \phi^s(Z^s)^{(N)} \Delta \hat{W}$$
$$z^{F(N+1)} = Z^F + \sum_N \phi^F(Z^F)^{(N)} \Delta \hat{U} \tag{4.4}$$

we have at each internal step n the following equality of nodal point coordinates

$$^n\hat{z}^s = {}^n\hat{z}^F \tag{4.5}$$

Solving the equation resulting from Eqs (4.4) and (4.5)

$$^n\hat{z}^s = Z^{*F} + \sum_N \phi^F({}^nZ^{*F})^{(N)} \Delta \hat{U} \tag{4.6}$$

we obtain a new coordinate $^{n+1}\hat{Z}^{*F}$ for the current fluid nodal point of the finite element.

This procedure is repeated until the following condition is satisfied

$$\Big|{}^{n+1}\hat{z}^s - {}^{n+1}\hat{z}^F\Big|^{(N+1)} \leqslant \varepsilon \tag{4.7}$$

where ε is sufficiently close to zero.

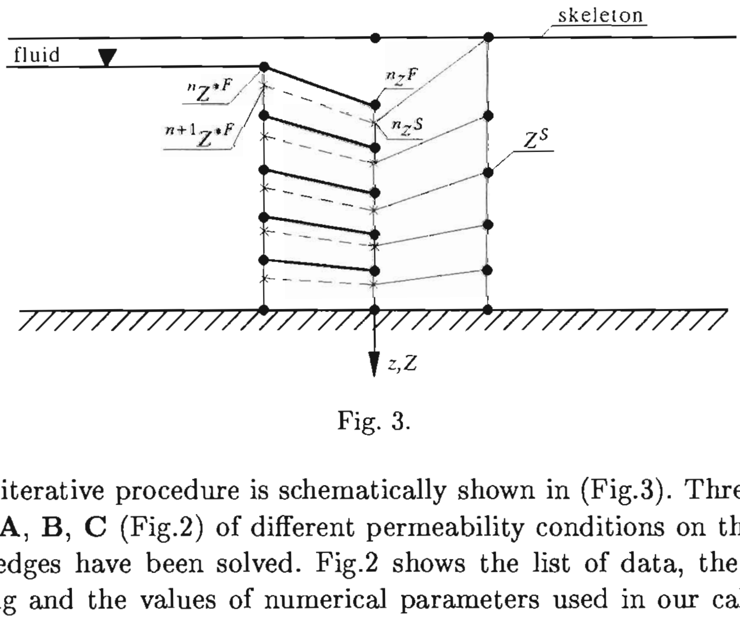

Fig. 3.

This iterative procedure is schematically shown in (Fig.3). Three kinds of subsoils **A**, **B**, **C** (Fig.2) of different permeability conditions on the top and bottom edges have been solved. Fig.2 shows the list of data, the character of loading and the values of numerical parameters used in our calculations.

The well-known in soil mechanics Krüger's formula for *permeability coefficient* describing its dependence on porosity is used.

$$k = \frac{2.8 \cdot 10^{-2} d_q n^3}{(1-n)^4} \tag{4.8}$$

where d_q – diameter of soil particles.

5. Conclusions

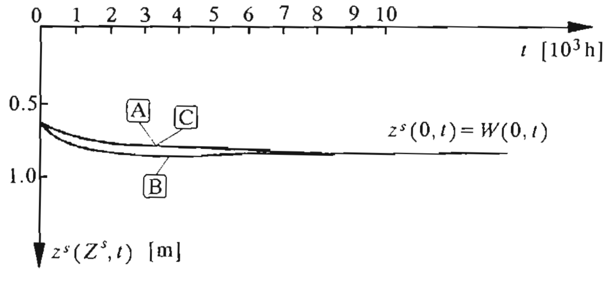

Fig. 4. Current position of the edge of upper layer (settlement)

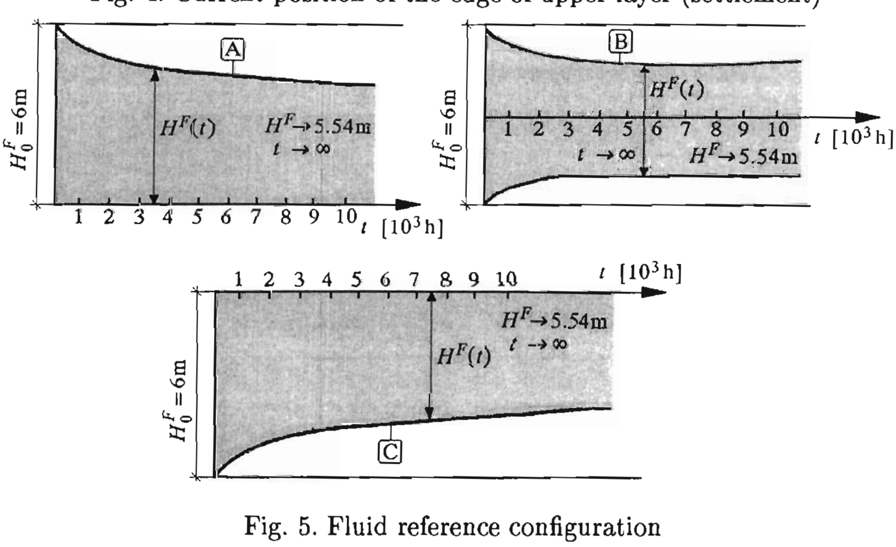

Fig. 5. Fluid reference configuration

The paper is summarized with the plots of: displacements of fluid and skeleton particles, current fluid reference configurations, porosity, permeability coefficient and fluid pressure distributions (see Fig.4 ÷ Fig.12).

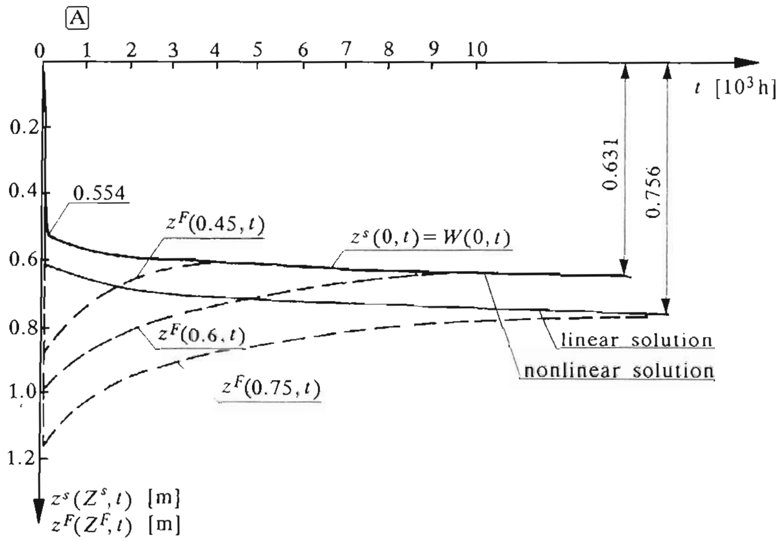
A
0 1 2 3 4 5 6 7 8 9 10
t [10³h]
0.2
0.4
0.6
0.8
1.0
1.2
0.554
zF(0.45, t)
zs(0, t) = W(0, t)
zF(0.6, t)
zF(0.75, t)
0.631
0.756
linear solution
nonlinear solution
zs(Zs, t) [m]
zF(ZF, t) [m]

Fig. 6.

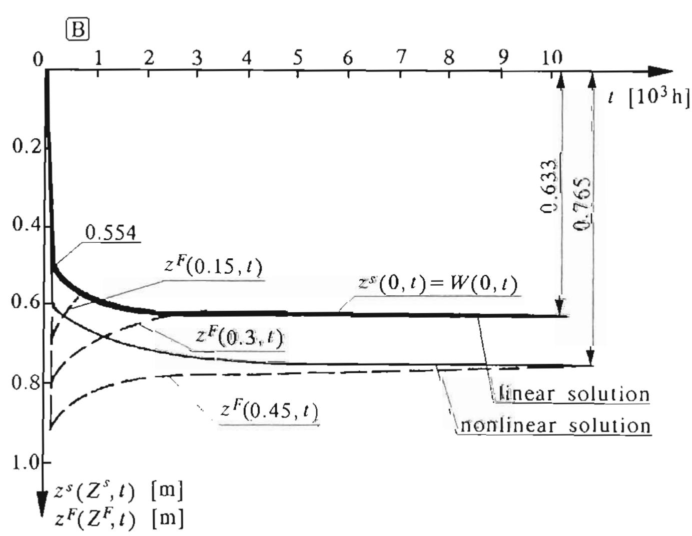
B
0 1 2 3 4 5 6 7 8 9 10
t [10³h]
0.2
0.4
0.6
0.8
1.0
0.554
zF(0.15, t)
zs(0, t) = W(0, t)
zF(0.3, t)
zF(0.45, t)
0.633
0.765
linear solution
nonlinear solution
zs(Zs, t) [m]
zF(ZF, t) [m]

Fig. 7.

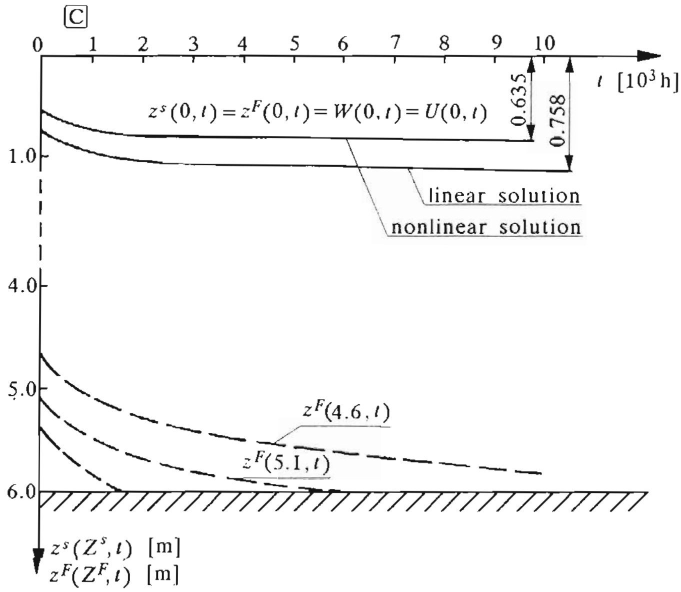
C
0 1 2 3 4 5 6 7 8 9 10
t [10³h]
0.635
0.758
z^s(0,t) = z^F(0,t) = W(0,t) = U(0,t)
1.0
linear solution
nonlinear solution
4.0
5.0
z^F(4.6,t)
z^F(5.1,t)
6.0
z^s(Z^s,t) [m]
z^F(Z^F,t) [m]

Fig. 8.

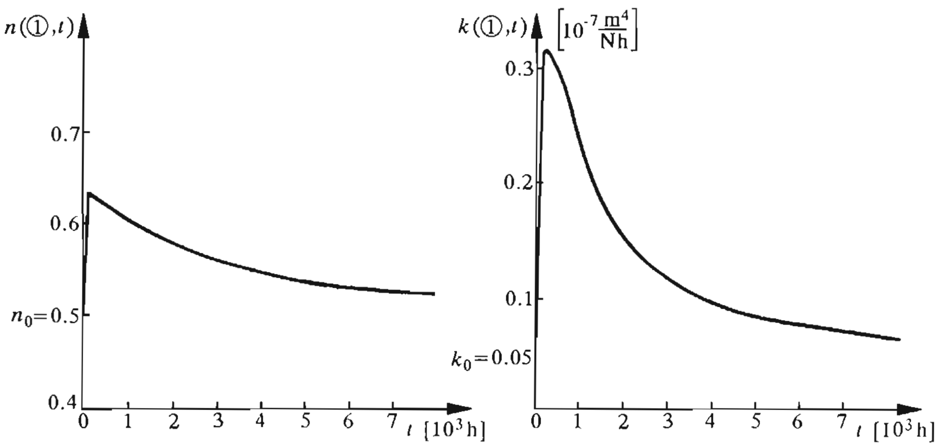
n(①,t)
0.7
0.6
n₀=0.5
0.4
0 1 2 3 4 5 6 7 t [10³h]
k(①,t) [10⁻⁷ m⁴/Nh]
0.3
0.2
0.1
k₀=0.05
0 1 2 3 4 5 6 7 t [10³h]

Fig. 9.

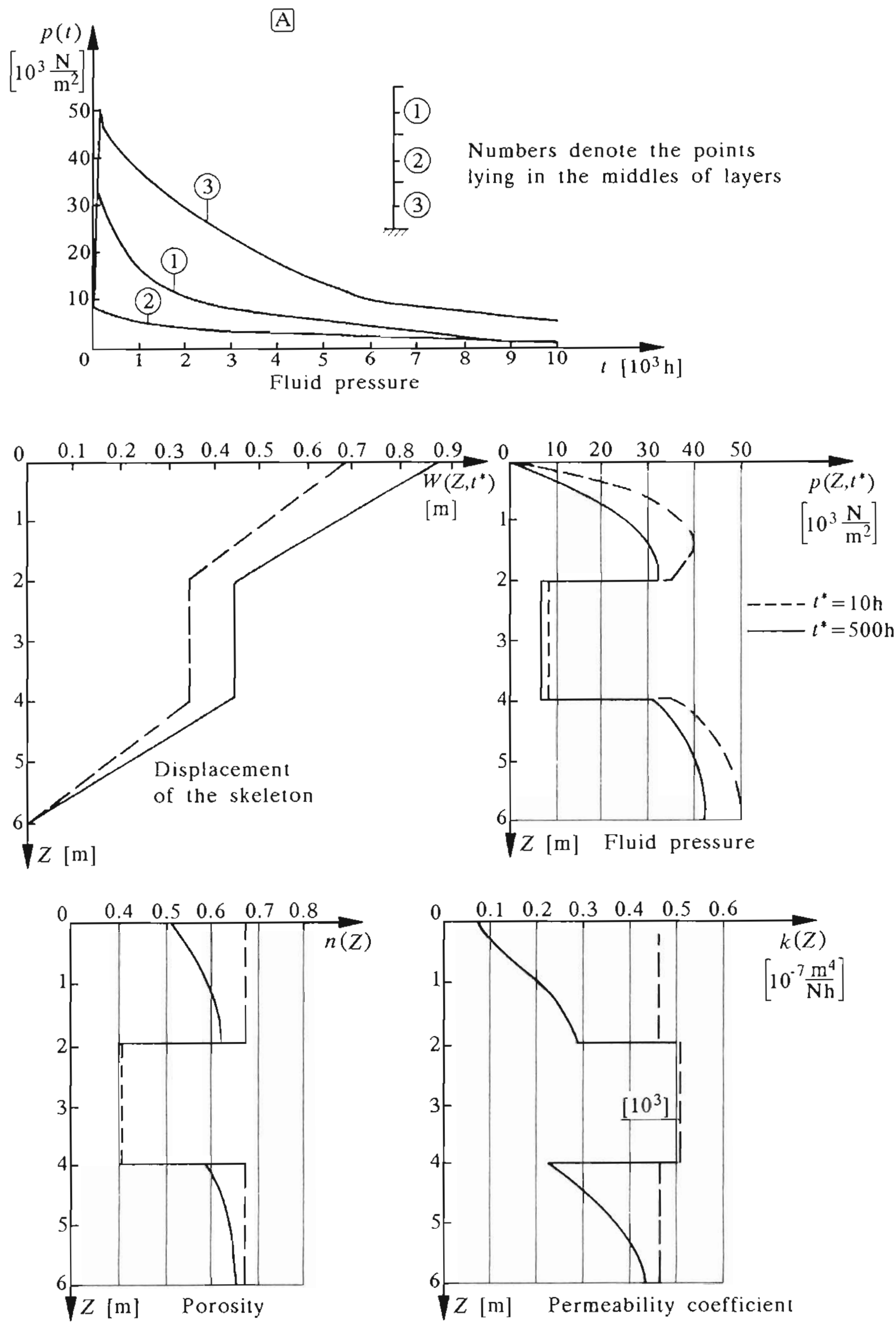

A
Numbers denote the points lying in the middles of layers
Fluid pressure
Displacement of the skeleton
Fluid pressure
t* = 10h
t* = 500h
Porosity
Permeability coefficient

Fig. 10.

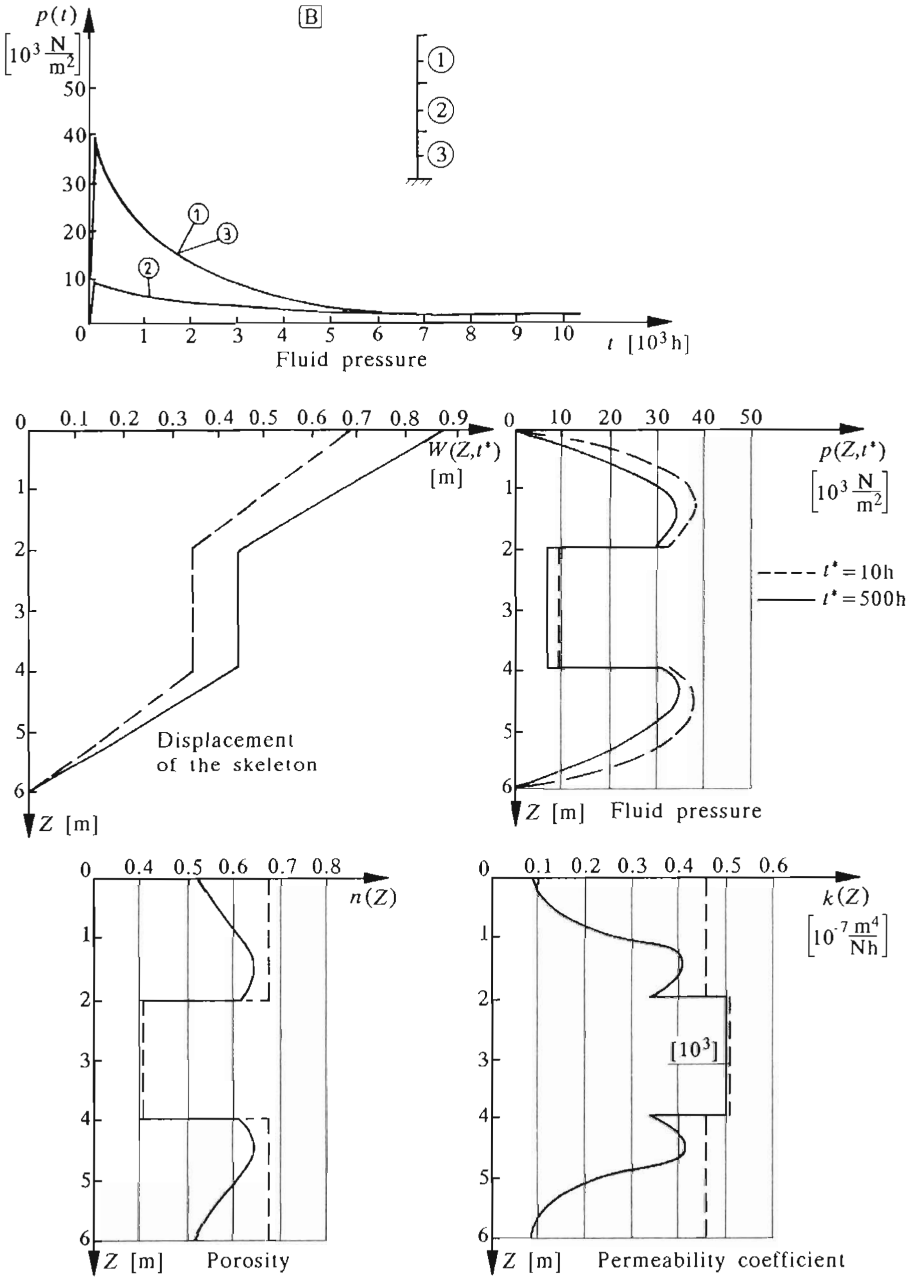
B
p(t)
[10³ N/m²]
Fluid pressure
t [10³h]
W(Z,t*) [m]
Displacement of the skeleton
Z [m]
p(Z,t*) [10³ N/m²]
t* = 10h
t* = 500h
Fluid pressure
n(Z)
Porosity
k(Z) [10⁻⁷ m⁴/Nh]
[10³]
Permeability coefficient

Fig. 11.

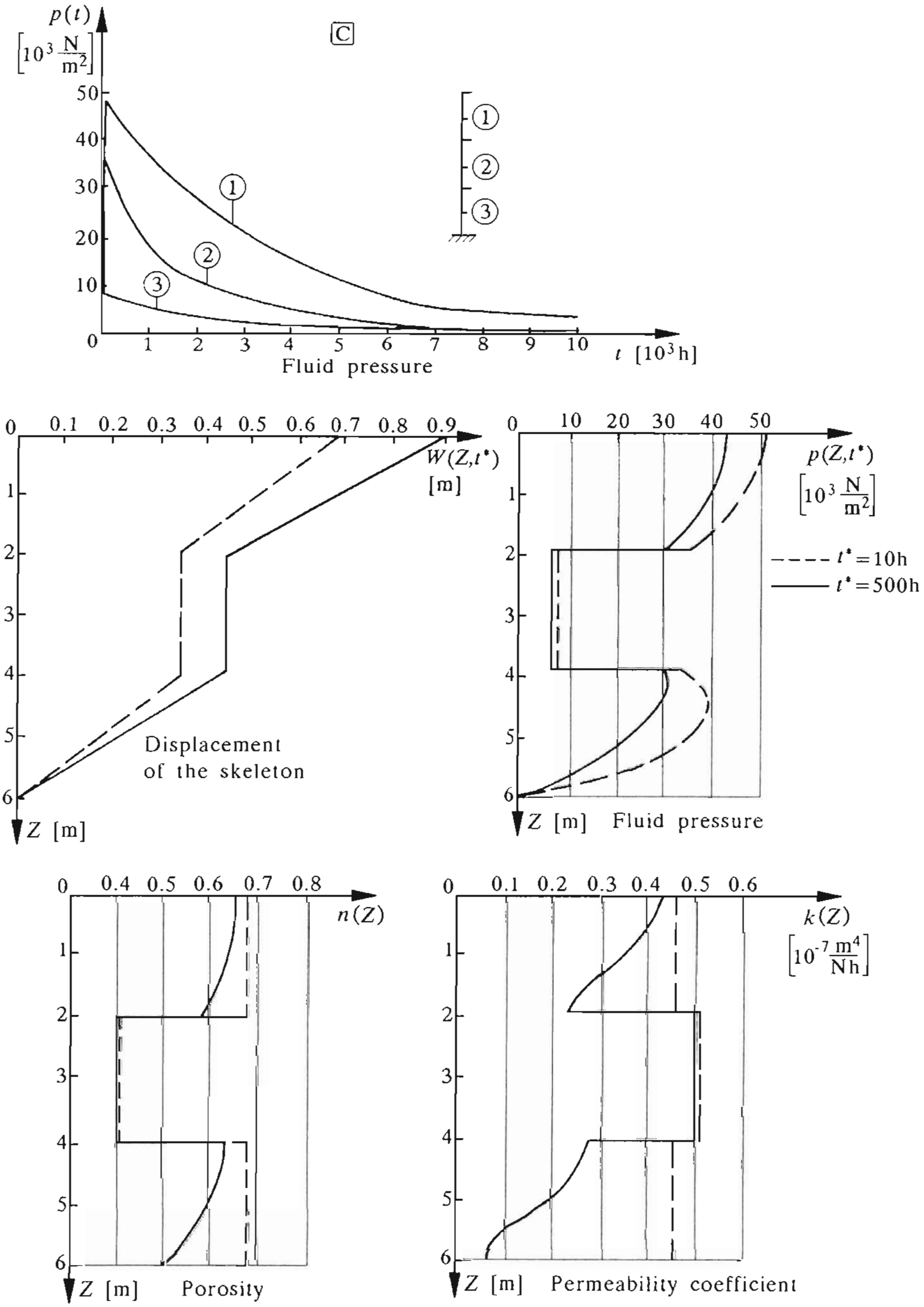

C
p(t)
[10³ N/m²]
t [10³h]
Fluid pressure
W(Z,t*) [m]
Displacement of the skeleton
Z [m]
p(Z,t*) [10³ N/m²]
t* = 10h
t* = 500h
Fluid pressure
n(Z)
Porosity
k(Z) [10⁻⁷ m⁴/Nh]
Permeability coefficient

Fig. 12.

In strongly deformable porous medium substantial changes of porosity and permeability can be seen. It is interesting that during rapid compression we observe initial increase in porosity (see Fig.9) and then it slowly decreases maintaining the level of external load.

Simultanously no essential difference in displacement distribution of the skeleton in the three kinds **A**, **B**, **C** of subsoils is observed. In some parts of the layers the value of fluid pressurre is about 25% of the value of external load (Fig.10 ÷ Fig.12), which means that this part of the load is carried by the fluid. Analysis of the paths of skeleton and fluid particles motion (Fig.6 ÷ Fig.8) allows for providing more precise description of the consolidation process and enables one to evaluate the amount of fluid squeezed out of the layers which can have a practical application to different porous bodies.

References

1. LEWIS R., SCHREFLER R., 1987, *The Finite Element Method in the Deformation and Consolidation of Porous Media*, J.Wiley, New York

2. MIKOŁAJEK M., 1990, Large Deformation of Porous Media (in Polish), *Proc. Committee of Appl. Mech. Polish Acad. Sci. - Mechanics*, **14**, Cracow

3. SZEFER G., 1980, Non-Linear Problems of Consolidation Theory, in: *Prob. Nonlin. de Mecanique*, PWN, Varsovie

4. SZEFER G., 1998, Computational Aspects of Saturated Porous Media Undergoing Large Deformations (a companion paper)

Konsolidacja wielowarstwowego podłoża porowatego w warunkach dużych deformacji

Streszczenie

W pracy rozważono proces deformacji porowatego szkieletu sprężystego przy skończonych odkształceniach oraz towarzyszącego transportu cieczy. W warunkach dużych deformacji te sprzężone zjawiska interakcji wymagają subtelnej analizy. Podano numeryczne rezultaty dla trójwarstwowego podłoża leżącego na sztywnym podkładzie przy różnych warunkach przepuszczalności w jednoosiowym stanie odkształcenia.

Manuscript received Fabruary 26, 1998; accepted for print April 20, 1998